The primary antimitotic mechanism of action of the synthetic halichondrin E7389 is suppression of microtubule growth

Mary Ann Jordan,[1] Kathryn Kamath,[1] Tapas Manna,[1] Tatiana Okouneva,[1] Herbert P. Miller,[1] Celia Davis,[1] Bruce A. Littlefield,[2] and Leslie Wilson[1]

[1]University of California Santa Barbara, Santa Barbara, California and [2]Eisai Research Institute, Andover, Massachusetts

Abstract

E7389, which is in phase I and II clinical trials, is a synthetic macrocyclic ketone analogue of the marine sponge natural product halichondrin B. Whereas its mechanism of action has not been fully elucidated, its main target seems to be tubulin and/or the microtubules responsible for the construction and proper function of the mitotic spindle. Like most microtubule-targeted antitumor drugs, it inhibits tumor cell proliferation in association with G_2-M arrest. It binds to tubulin and inhibits microtubule polymerization. We examined the mechanism of action of E7389 with purified microtubules and in living cells and found that, unlike antimitotic drugs including vinblastine and paclitaxel that suppress both the shortening and growth phases of microtubule dynamic instability, E7389 seems to work by an end-poisoning mechanism that results predominantly in inhibition of microtubule growth, but not shortening, in association with sequestration of tubulin into aggregates. In living MCF7 cells at the concentration that half-maximally blocked cell proliferation and mitosis (1 nmol/L), E7389 did not affect the shortening events of microtubule dynamic instability nor the catastrophe or rescue frequencies, but it significantly suppressed the rate and extent of microtubule growth. Vinblastine, but not E7389, inhibited the dilution-induced microtubule disassembly rate. The results suggest that, at its lowest effective concentrations, E7389 may suppress mitosis by directly binding to microtubule ends as unliganded E7389 or by competition of E7389-induced tubulin aggregates with unliganded soluble tubulin for addition to growing microtubule ends. The result is formation of abnormal mitotic spindles that cannot pass the metaphase/anaphase checkpoint. [Mol Cancer Ther 2005;4(7): 1086–95]

Introduction

Halichondrin B (Fig. 1) is a large polyether macrolide found in a number of marine sponges. It was shown to inhibit the proliferation of tumor cells with high potency, and strong evidence indicates that it acts by blocking cell cycle progression at G_2-M by an action on tubulin or microtubules (1). *In vitro*, halichondrin B noncompetitively inhibits the binding of vinblastine to tubulin, indicating that it may bind to tubulin in the *Vinca* binding domain (2), and it inhibits the polymerization of tubulin into microtubules.

E7389, currently in phase I and II clinical trials, is a synthetic derivative of halichondrin B that is simpler in structure than the parent compound but retains the potency of halichondrin B (Fig. 1). The complete chemical synthesis of E7389 represents a major advance, eliminating the economic and ecological problems inherent in obtaining ample quantities of potential drugs from natural sources. E7389 strongly inhibits growth of a number of human tumor xenografts in mice, and like halichondrin B, it induces G_2-M cell cycle arrest, disrupts mitotic spindle organization, and induces apoptosis in tumor cells (3, 4). Recent evidence indicates that E7389 binds to tubulin and inhibits the polymerization of bovine brain tubulin into microtubules at micromolar concentrations (3). However, when compared with other microtubule-targeted classes of drugs, the halichondrins exhibit a unique constellation of effects on the conformation of tubulin as indicated by their effects on tubulin alkylation, on the chemical cross-linking of tubulin, and on the binding to tubulin of the hydrophobic probe, bis-8-anilinonaphthalene sulfate (5). Such data have led to the idea that the halichondrins interact with tubulin in a manner distinct from that of other microtubule-targeted drugs and, thus, that they might possess unique antitumor activities (3).

Whereas the target for the halichondrins in general, and for E7389 in particular, seems to be tubulin and/or microtubules, the way in which these compounds perturb microtubule polymerization and/or dynamics both in cell-free systems and in cells has not been determined. Antimitotic drugs can interact with tubulin and microtubules in a large number of distinct ways to disrupt microtubule polymerization and dynamics, and their distinct mechanisms may be important determinants of their specific anticancer activities (6). Microtubules are highly dynamic polymers and their dynamics, which are critically important for many cellular processes, are tightly regulated both spatially and temporally (6, 7). In one form of microtubule dynamics, called ''dynamic instability,'' the

Received 12/21/04; revised 4/1/05; accepted 5/4/05.

Grant support: Eisai Research Institute and NIH grants CA 57291 and NS13560.

The costs of publication of this article were defrayed in part by the payment of page charges. This article must therefore be hereby marked advertisement in accordance with 18 U.S.C. Section 1734 solely to indicate this fact.

Requests for reprints: Mary Ann Jordan, Molecular, Cellular, and Developmental Biology, University of California Santa Barbara, Santa Barbara, CA 93106-9610. Phone: 805-893-5317; Fax: 805-893-4724. E-mail: jordan@lifesci.ucsb.edu

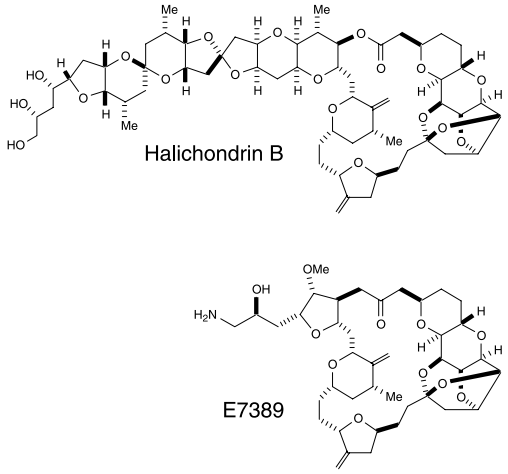

Figure 1. Structures of E7389 and halichondrin.

individual microtubule ends undergo frequent stochastic transitions between episodes of growth and shortening (8). Dynamic instability plays a critical role in the assembly and function of the mitotic spindle and, thus, in cell proliferation (6, 7). Specifically, dynamically unstable microtubules are required for the proper attachment of chromosomes to the spindle, for proper alignment of the chromosomes at metaphase (congression), and for signaling and induction of their subsequent separation at anaphase.

Many antimitotic anticancer drugs that destabilize microtubules and suppress the dynamics of microtubules seem to inhibit mitosis at the metaphase/anaphase transition by binding directly to the microtubules and suppressing both the growth and shortening phases of microtubule dynamics (6, 9–15). The cells are unable to pass the mitotic cell cycle checkpoint and to initiate anaphase movements, or do so only after a long period of mitotic blockage, apparently due to their suppressed microtubule dynamics. Cells ultimately die by apoptosis, which occurs either directly after mitotic arrest or after aberrant exit from mitosis into a multinucleate interphase (4, 16–18).

To further elucidate the mechanism of action of E7389, we have examined its effects on the structure of microtubules and of nonmicrotubule polymers formed when tubulin is polymerized into microtubules in the presence of the compound. We have also determined its effects on the dynamic instability of microtubules both *in vitro* with purified microtubules and in living MCF7 cells. We find that E7389 suppresses dynamic instability of microtubules in living interphase MCF7 cells at the same concentrations that block cell proliferation and induce mitotic arrest in the cells. In contrast to both microtubule-stabilizing drugs, such as taxol, epothilone B, and discodermolide, and microtubule-destabilizing drugs, such as vinblastine, mitotic block by E7389 involves suppression of microtubule growth events, with no effect on the shortening events. The effects of E7389 on dynamic instability *in vitro* were qualitatively similar to those produced in living cells, and also occurred concomitant with aggregation of the tubulin, as determined by electron microscopy. The results are consistent with an end-poisoning mechanism in which, at its lowest effective concentrations, E7389 suppresses mitosis primarily by binding to microtubule ends itself or by competition of E7389-induced tubulin aggregates with unliganded soluble tubulin for addition to growing microtubule ends.

Materials and Methods

Materials

E7389 [NSC-707389; previously ER-086526; CA index: 11,15:18,21:24.28-triepoxy-7,9-ethano-12,15-methano-9*H*,15*H*-furo[3,2-*i*]furo[2′,3′:5,6]pyrano[4,3-b][1,4]dioxacyclopentacosin-5-(4*H*)-one, 2-[(2*S*)-3-amino-2-hydroxypropyl]hexacosahydro-3-methoxy-26-methyl-20,27-bis(methylene)-, (2*R*,3*R*,3a*S*,7*R*,8a*S*,9*S*,10a*R*,11*S*,12*R*,13a*R*,13b*S*,15*S*,18*S*,21*S*,24*S*,26*R*,28*R*,29a*S*)-] was synthesized at Eisai Research Institute (19).

Purification of Microtubule Protein and Tubulin

Bovine brain microtubule protein consisting of ~70% tubulin and 30% microtubule-associated proteins (MAP) was isolated without glycerol by three cycles of polymerization and depolymerization. Tubulin was purified from the microtubule protein preparation by phosphocellulose chromatography, frozen in liquid nitrogen, and stored at −70°C (20). On the day of use, the tubulin was thawed on ice and centrifuged (17,000 × *g*, 20 minutes, 4°C) to remove aggregated or denatured tubulin. Protein concentration was determined by the Bradford (21) assay using bovine serum albumin as the standard.

Inhibition of Microtubule Polymerization

Microtubule-nucleating seeds were prepared by assembling tubulin (2.5 mg/mL) in PEM (100 mmol/L PIPES, 1 mmol/L EGTA, and 1 mmol/L $MgSO_4$, pH 6.8) plus 10% DMSO and 10% glycerol and 1 mmol/L GTP, then shearing the microtubules several times through a 25-gauge needle. Purified tubulin (1.5–2.9 mg/mL) in PMME (87 mmol/L PIPES, 36 mmol/L 2-morpholinoethanesulfonic acid, 1.8 mmol/L $MgCl_2$, 1 mmol/L EGTA, pH 6.8) containing 2.0 mmol/L GTP was assembled by mixing with seeds (1:50 dilution, seed/tubulin) and the stated concentration of E7389 and incubating at 37°C for 60 minutes in a temperature-controlled Gilford Response spectrophotometer. Polymerization was determined from the absorbance at 350 nm.

Electron Microscopy

Microtubules assembled from MAP-depleted bovine brain tubulin (2.5 mg/mL) and a range of concentrations of E7389 (60 minutes) were fixed (15 minutes, 1% glutaraldehyde) and applied to carbon/formvar-coated electron microscope grids for ~90 seconds. Excess fluid was drawn off using torn edges of filter paper and was sequentially followed by a 15-second application of cytochrome *c* (1 mg/mL), washing (3 drops of water), and a 20-second application of uranyl acetate (drawn off). Images were collected using a JEOL 1230 electron microscope (80 kV).

Analysis of Microtubule Dynamic Instability *In vitro*

Tubulin (15 μmol/L) was polymerized onto nucleating flagellar seeds in PMME buffer containing 1 mmol/L GTP (37°C) for 30 minutes to reach polymer mass steady state in the absence or presence of E7389. Samples of microtubule suspensions (4 μL) were prepared for video microscopy and the dynamics of individual microtubules were recorded (37°C) and analyzed as described elsewhere (22). Microtubules were observed for a maximum of 60 minutes after reaching steady state. At the experimental conditions used, microtubule growth occurred predominantly at the plus ends of the seeds as determined by the growth rates, the number of microtubules that grew, and the relative lengths of the microtubules at the opposite ends of the seeds (23–26). We considered a microtubule to be in a growth phase if it increased in length by >0.2 μm at a rate of >0.2 μm/min, and in a shortening phase if it shortened by >0.2 μm at a rate of >0.3 μm/min. Microtubules undergoing length changes of ≤0.2 μm over the duration of six data points were considered to be in an attenuated or paused state. The same tubulin preparation was used for all dynamics experiments; 20 to 30 microtubules were analyzed for each experimental condition.

The catastrophe frequency (a catastrophe is a transition from the growing or attenuated state to shortening; ref. 25) was determined by dividing the number of catastrophes by the sum of the total time spent in the growing plus attenuated states for all microtubules for a particular experimental condition. The rescue frequency (a rescue is a transition from shortening to growing or attenuation, excluding new growth from a seed; ref. 25) was calculated by dividing the total number of rescue events by the total time spent shortening for all microtubules at a particular experimental condition. Dynamicity is the sum of all growing and shortening events divided by the total time measured, including time spent in the attenuated state. SDs for dynamic parameters were determined as described in ref. 25.

Effects of E7389 on the Dilution-Induced Disassembly of Microtubules: Comparison with Vinblastine

Microtubules were prepared by assembling MAP-rich microtubule protein (2.7 mg/mL, 30°C, 60 minutes) in PEM buffer containing a GTP-regenerating system [1.5 IU/mL acetate kinase, 10 mmol/L acetyl phosphate, and 0.1 mmol/L GTP ([^{3}H]GTP; final specific activity, 75 Ci/mol)]. MAP-rich microtubules were used to facilitate collection of the microtubules on glass fiber filters (27). The mean microtubule length was determined by electron microscopy of samples fixed in 0.2% glutaraldehyde and negatively stained with 1.5% uranyl acetate. The microtubule solutions were divided into three tubes. After assembly, vinblastine (1.4 μmol/L), E7389 (4 μmol/L), or an equivalent volume of buffer was added to each tube. The drug concentrations were chosen because, under the conditions used, they inhibited microtubule polymerization by 30% as determined by turbidimetry (data not shown). One minute after drug addition, aliquots of the suspensions (0.5 mL) were diluted 15-fold by rapid mixing with 7.0 mL of dilution buffer (30°C) containing 1.4 μmol/L vinblastine or 4 μmol/L E7389 or no drug. Samples were removed (0.6 mL) at 10-second intervals and stabilized immediately in 19.4 mL stabilization buffer (30°C). Radiolabel retention by the microtubules was determined after trapping the microtubules on glass fiber filters. Tubulin loss rates per microtubule were calculated by determining the time dependence for retention of [^{3}H]GDP in the microtubules after dilution.

Determination of Dynamic Instability in the Thin Peripheral Regions of Living Interphase MCF7 Cells

MCF-7 cells stably transfected with green fluorescent protein-α-tubulin (Clontech, Palo Alto, CA) were seeded onto glass coverslips treated with 50 μg/mL poly-L-lysine, 10 μg/mL laminin, and 20 μg/mL fibronectin (2 hours, 37°C, washed once with sterile water; Gibco, Carlsbad, CA) to enhance flattening. Six hours after adding E7389, the growth and shortening of microtubules in cells maintained at 36 ± 1°C was recorded by time-lapse fluorescence microscopy using a Hamamatsu Orca II digital camera driven by Metamorph software. The positions of the plus ends of microtubules were tracked and graphed as a function of time. Changes of ≥0.5 μm between two points were considered growth or shortening events. Changes in length of <0.5 μm were considered periods of attenuated dynamics or pause. Results were obtained from >70 individual microtubules from 15 or more cells for each condition.

Determination of Cell Proliferation and Mitotic Arrest

Human MCF-7 breast cancer cells from the American Type Culture Collection (Rockville, MD) were cultured in media containing standard glucose DMEM (Sigma Chemical, St. Louis, MO), 5% fetal bovine serum (HyClone, Logan, UT), 1% penicillin-streptomycin, supplemental glutamine and nonessential amino acids, and sodium bicarbonate, pH 7.3 (37°C; Sigma) in the presence of 5% carbon dioxide. Cells seeded at 6×10^4 cells/2 mL in six-well plates were allowed to adhere (24 hours) before the incubation medium was replaced by medium including drug. For determination of inhibition of proliferation, cells were incubated with a range of E7389 concentrations for 20 hours, rinsed with Versene (137 mmol/L NaCl, 2.7 mmol/L KCl, 1.5 mmol/L KH_2PO_4, 8.1 mmol/L Na_2HPO_4, 0.5 mmol/L EDTA), detached with trypsin (0.5 mg/mL in PBS: 137 mmol/L NaCl, 2.7 mmol/L KCl, 1.5 mmol/L KH_2PO_4, 8.1 mmol/L Na_2HPO_4, and 0.5 mmol/L EDTA, pH 7.2), stained with trypan blue, and counted by hemacytometer. Results are averages of five independent experiments.

For determination of mitotic block, cells were incubated with E7389 for 20 hours and collected as above for fixation in 10% formalin (25°C) followed by methanol (4°C). Fixed cells were fluorescently stained for chromatin and chromosomes with 4′,6-diamidino-2-phenylindole and with antibodies to α-, β-, and γ-tubulin (Abcam, Cambridge, MA, and Sigma), mounted on slides, and examined by fluorescence microscopy (Nikon Eclipse E800, Melville, NY); the percentage of cells in mitosis was determined.

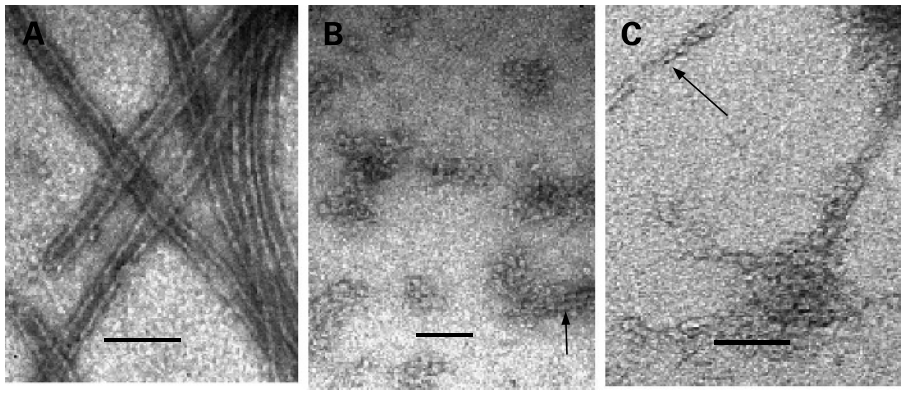

Figure 2. E7389-induced formation of tubulin aggregates as determined by electron microscopy. **A**, no drug, microtubules with no significant aggregated tubulin. **B**, 1 μmol/L E7389, the number of microtubules decreased and there were large numbers of aggregates of globular tubulin subunits (*arrows*). **C**, 3.3 μmol/L E7389, globular aggregates and sheets (not shown) were present.

Results

E7389 Concentrations ≥100 nmol/L Prevent Microtubule Polymerization and Induce Formation of Globular Tubulin Aggregates *In vitro*

Microtubules were polymerized to steady state with MAP-depleted bovine brain tubulin in the presence or absence of a range of E7389 concentrations, and the mass of assembled microtubule polymer was determined by turbidimetry (Materials and Methods). E7389 (100 nmol/L) inhibited microtubule polymerization by 4.7 ± 1.3%, 330 nmol/L E7389 inhibited polymerization by 12.1 ± 1.8%, and 1 μmol/L E7389 inhibited polymerization by 46.9 ± 2.4%. Thus, E7389 inhibits microtubule polymerization in a concentration-dependent manner.

The structure of the microtubules formed from MAP-depleted tubulin in the presence of E7389 and any tubulin aggregation were assessed by electron microscopy. Control microtubules were normal in appearance, and the suspensions contained little or no detectable aggregated protein (Fig. 2A). Whereas E7389 did not alter the structure of the microtubules that formed in the presence of the compound, it did induce the formation of unusual tubulin aggregates. At E7389 concentrations that significantly reduced the microtubule polymer mass (330 nmol/L and 1 μmol/L), the number of microtubules decreased, and a few globular aggregates and rare filaments were formed (Fig. 2B). However, as the E7389 concentration was increased to 3.3 μmol/L (Fig. 2C) and even higher to 10 μmol/L, the amount of tubulin aggregation increased substantially, some sheets were formed (data not shown), and the quantity of microtubules substantially decreased. Very few microtubules formed at E7389 concentrations ≥3.3 μmol/L. At E7389 concentrations >10 μmol/L, only sheets and small aggregates were detected. The individual particles in the aggregates were ellipsoid in shape and measured 24 ± 6 nm (SD) in length and 14 ± 4 nm (SD) in width (n = 20).

E7389 Primarily Inhibits the Growth Parameters of Steady-State Microtubule Dynamic Instability *In vitro*

We analyzed the effects of E7389 on the dynamic instability behavior of individual reassembled MAP-free bovine brain microtubules at their plus ends *in vitro* at steady state. Life history traces showing the changes in length of the microtubules in the absence and presence of 100 nmol/L E7389 are shown in Fig. 3. The plus ends of control microtubules (Fig. 3A) grew relatively slowly, shortened relatively rapidly, and occasionally persisted in an attenuated (paused) state, neither growing nor shortening detectably. As shown in Fig. 3B, 100 nmol/L E7389 clearly reduced the growth rate and increased the fraction of time the microtubules spent in an attenuated or paused state but had little apparent effect on the shortening rate.

The dynamic instability parameters quantitatively determined from such life history plots in the absence and

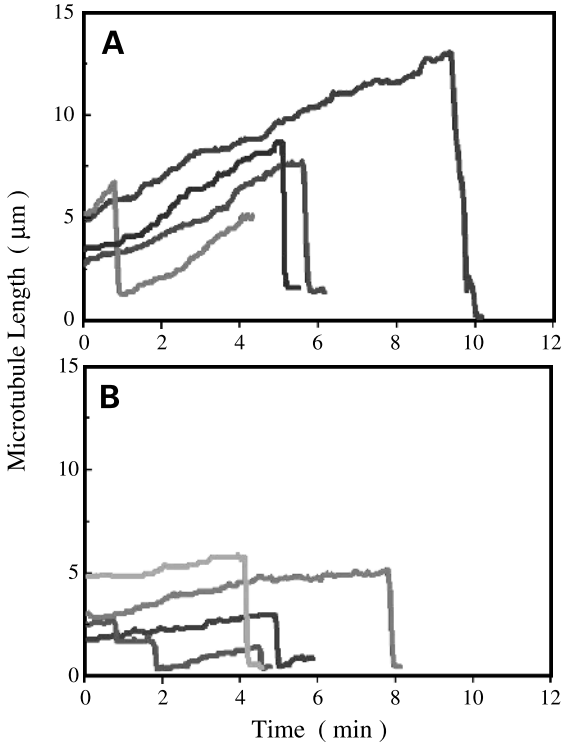

Figure 3. Life history traces of microtubules assembled *in vitro* from bovine brain tubulin. **A**, controls. **B**, 100 nmol/L E7389. Growth rates and lengths are suppressed by E7389 and microtubules spend a significantly greater amount of time in a state of pause or attenuated dynamics.

Table 1. Suppression of dynamic instability at microtubule plus ends by E7389 *in vitro* and in living cells at the concentration that induced half-maximal mitotic arrest (1 nmol/L)

	In vitro			In living MCF7 cells		
	Control	E7389, 100 nmol/L	Percent change	Control	E7389, 1.0 nmol/L	Percent change
Growth rate (μm/min)	0.90 ± 0.07	0.49 ± 0.04*	−46	13.3 ± 0.4	9.7 ± 0.4*	−27
Growing length (μm)	2.39 ± 0.32	1.18 ± 0.16*	−51	4.2 ± 0.3	2.1 ± 0.2*	−50
Growing duration (min)	2.7 ± 0.3	2.5 ± 0.3	ns	0.32 ± 0.02	0.23 ± 0.01*	−28
Shortening rate (μm/min)	32.9 ± 1.9	24.4 ± 1.9†	†	26.3 ± 1.2	27.0 ± 1.2	ns
Shortening length (μm)	5.89 ± 0.54	3.67 ± 0.38†	†	6.1 ± 0.5	5.1 ± 0.4	ns
Shortening duration (min)	0.18 ± 0.01	0.16 ± 0.01	ns	0.2 ± 0.01	0.18 ± 0.01	ns
Attenuation (pause) duration (min)	0.95 ± 0.12	1.18 ± 0.17	ns	0.27 ± 0.02	0.31 ± 0.02	ns
% Time growing	84.9%	74.1%		39.5	28.2	
% Time shortening	5.0%	4.6%		19.4	15.4	
% Time attenuated	10.1%	21.3%		41.1	55.4	
Catastrophe frequency per minute	0.29	0.30	ns	1.1 ± 0.92	1.0 ± 0.6	ns
Rescue frequency per minute	2.37	2.21	ns	4.7 ± 2.8	5.4 ± 3.7	ns
Dynamicity	2.37	1.43	−40	10.4 ± 4.7	7.5 ± 4.1*	−28

NOTE: Values given are mean ± SE, except for dynamicity which is ± SD; ns, not significant. Catastrophe and rescue frequencies in living cells were also calculated on the basis of events per length grown or shortened and did not differ in the presence or absence of 1.0 nmol/L E7389 (data not shown). Catastrophe and rescue frequencies are presented on a per microtubule basis in living cells and on an overall basis *in vitro*. *In vitro*, between 26 and 30 growth events and between 25 and 26 shortening events were measured for each condition. In living cells, the measurements were made for 15 to 19 different cells and for 73 to 97 different microtubules for each condition.

*Values differ significantly from controls at the 99% confidence levels by Student's *t* test.

†Shortening rates were not considered reliable *in vitro* because the shortening lengths were reduced artifactually by the significantly shorter overall lengths of the microtubules, making it difficult to measure them accurately.

presence of 100 nmol/L E7389 are shown in Table 1 (columns 1–4). This relatively low concentration of E7389 strongly suppressed the rate and extent of growth and the overall dynamicity of the microtubules. Specifically, E7389 suppressed the growth rate by 46%, from 0.9 to 0.49 μm/min, and suppressed the length grown during a growth event by 51%, from 2.39 to 1.18 μm. It more than doubled the percentage of time the microtubules remained in an attenuated state (from 10.1% to 21.3%), and it suppressed the dynamicity by 40%. Other parameters were not significantly affected. For example, dynamic instability is characterized by abrupt stochastic transitions among the phases of growth, shortening, and pause, called ''catastrophes'' and ''rescues'' (Materials and Methods). The catastrophe and rescue frequencies were unchanged by 100 nmol/L E7389. At concentrations >100 nmol/L, microtubules were so short that their dynamics could not be measured. Overall, these data indicate that the principal effect of E7389 on microtubules *in vitro* is to inhibit the rate and extent of microtubule growth.

Most microtubule-active drugs we have examined to date have significantly suppressed one or another component of microtubule shortening (for review, see ref. 9). E7389 (100 nmol/L) reduced the shortening rate by 26% (Table 1). We were concerned about the significance of this finding; the measurements were very difficult to make because the microtubules at steady state in the presence of 100 nmol/L E7389 were very short, leading to the possibility of large measurement error. (The mean length of the microtubules decreased from 5.2 ± 3.6 μm in controls to 2.8 ± 1.5 μm in the presence of 100 nmol/L E7389.) The shortened length of the microtubules made the determination of shortening rates uncertain, and artifactually reduced the value for ''length shortened.'' Because the microtubules were even shorter at higher concentrations of E7389, it also was not possible to raise the E7389 concentration. Thus, we turned to another experimental method. To more closely examine whether E7389 could affect microtubule shortening, we examined the effects of the drug on the disassembly rate by dilution-induced disassembly of MAP-rich microtubules uniformly radiolabeled with [^{3}H]GTP (Materials and Methods). Dilution of microtubules by 15-fold as carried out here reduces the soluble tubulin concentration to a level far below the critical subunit concentration required for growth at either microtubule end and, thus, the apparent tubulin dissociation rate constant at the combined microtubule ends can be readily analyzed in the absence of any tubulin association. The effects of E7389 on the dilution-induced rate of disassembly and the effects of vinblastine for comparison were measured by collecting the disassembling microtubules every 10 seconds during a 90-second dilution into a stabilizing buffer containing either 4 μmol/L E7389, 1.4 μmol/L vinblastine, or no drug. The drug concentrations chosen were those that inhibited MAP-rich microtubule polymerization by 30% of control under the conditions of the experiment. In the absence of drug, microtubules disassembled at an average rate of 37 ± 3 dimers/microtubule/s. Figure 4 shows the averaged results of several experiments. Over the period of 15 to 120 seconds after dilution, the rate of loss of polymer mass was

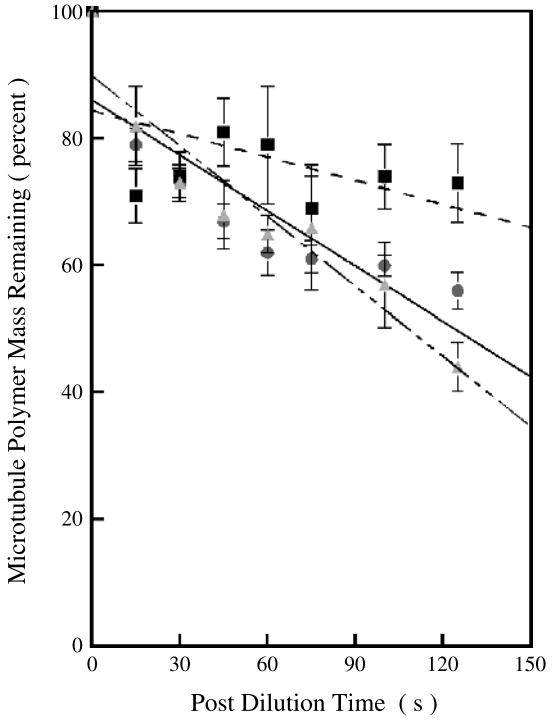

Figure 4. Effects of E7389 (4 μmol/L, ▲) and vinblastine (1.4 μmol/L, ■) on the rate of dilution-induced disassembly of microtubules. E7389 had no stabilizing effect on the off-rate constant as compared with control (●), whereas vinblastine significantly reduced the off-rate constant (by 59%). Radiolabeled microtubules were assembled to steady state, as described in Materials and Methods, and divided into three aliquots. E7389, vinblastine, or an equivalent volume of buffer was added to each aliquot and 1 min later, the microtubules were diluted 15-fold into buffer containing the same concentration of drug or no drug to induce disassembly. Samples of each reaction were stabilized at 10-s intervals for analysis of retained label by filter assay. *Points,* mean for each time point from four experiments for control and E7389 and three experiments for vinblastine; *bars,* SE.

0.29%/s for control microtubules, 0.37%/s for 4 μmol/L E7389, and only 0.12%/s for 1.4 μmol/L vinblastine. Thus, vinblastine reduced the disassembly rate by 59%, but E7389 did not reduce it at all. The results indicate that, in strong contrast to vinblastine which significantly stabilizes microtubules against dilution-induced depolymerization, E7389 has little or no effect on the tubulin off-rate constant at either microtubule end.

E7389 Blocked Mitosis in MCF-7 Cells in Concert with Inhibition of Proliferation

As shown in Fig. 5, after 20 hours of incubation, E7389 (1 nmol/L) induced half-maximal accumulation of cells in mitosis, and maximal mitotic accumulation (39%) occurred at concentrations of 10 nmol/L and above. E7389 also inhibited the proliferation of MCF7 cells at approximately the same concentration that blocked mitosis by 50%. At approximately the concentration for half-maximal mitotic block, MCF7 cell proliferation was inhibited by 50% (IC_{50}, 1.5 nmol/L), indicating that mitotic arrest is a principal mechanism of inhibition of proliferation by E7389.

E7389 Suppresses Microtubule Growth Dynamics in Living MCF7 Cells

After stable transfection of MCF7 cells with green fluorescent protein-tubulin, the dynamic instability behavior of the fluorescently labeled microtubules in the thin lamellar edge of cells during interphase can be readily imaged by time-lapse microscopy (Materials and Methods). Figure 6A shows the lamellar region of a living, untreated MCF7 cell expressing green fluorescent protein-tubulin observed at 4-second intervals. Consistent with results in many cell types, microtubules continuously alternated between phases of growing, shortening, and a paused state (a state of attenuated or undetectable dynamic activity). The life history plots show the positions of individual microtubule plus ends over time (Fig. 6B and C); these graphs were used to determine the parameters of dynamic instability (Table 1, *right columns*). In control MCF7 cells (Fig. 6B), microtubules shortened at a mean rate of 26.3 μm/min, faster than their mean growing rate of 13.3 μm/min. They spent 39.5% of the time growing, 19.4% of the time shortening, and 41.1% of the total time in a phase of pause or attenuated dynamics. As shown in the life history plot (Fig. 6C) and in Table 1, 1 nmol/L E7389 (the concentration that inhibited mitosis half-maximally) suppressed the rate, duration, and extent of growing excursions and the overall dynamicity. In agreement with the results obtained *in vitro* with purified microtubules (Table 1; Fig. 4), E7389 did not affect the shortening dynamics. The growth rate was inhibited by 27%, the growth duration by 28%, the length grown by 50%, and the dynamicity by 28%. There was virtually no effect of E7389 on any of the shortening parameters or the frequencies of catastrophe or rescue (Table 1).

At 2 nmol/L E7389 (twice the concentration that induced half-maximal mitotic accumulation), dynamic instability in the thin peripheral regions of the cells was further suppressed. At this concentration, microtubule dynamicity varied from cell to cell. Of 23 cells examined, in 15 cells the majority of microtubules were so minimally dynamic that their dynamics could not be accurately measured.

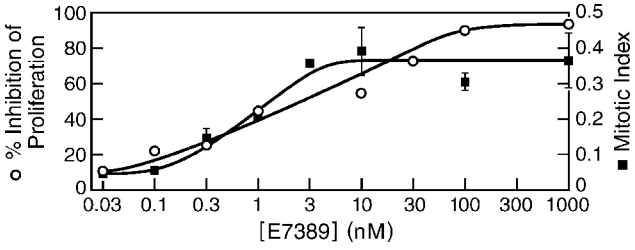

Figure 5. Concentration dependence for inhibition of MCF7 cell proliferation (72 h; ○) and for mitotic index (20 h; ■) by E7389. To determine proliferation, cells were incubated with E7389 (0.033 nmol/L – 1 μmol/L) for 72 h and counted by hemacytometer after trypan blue staining (Materials and Methods). To determine mitotic index, cells were incubated with E7389 for 20 h, fixed, and stained with 4′,6-diamidino-2-phenylindole to visualize nuclei (Materials and Methods). *Points,* mean of three to four experiments; *bars,* SD.

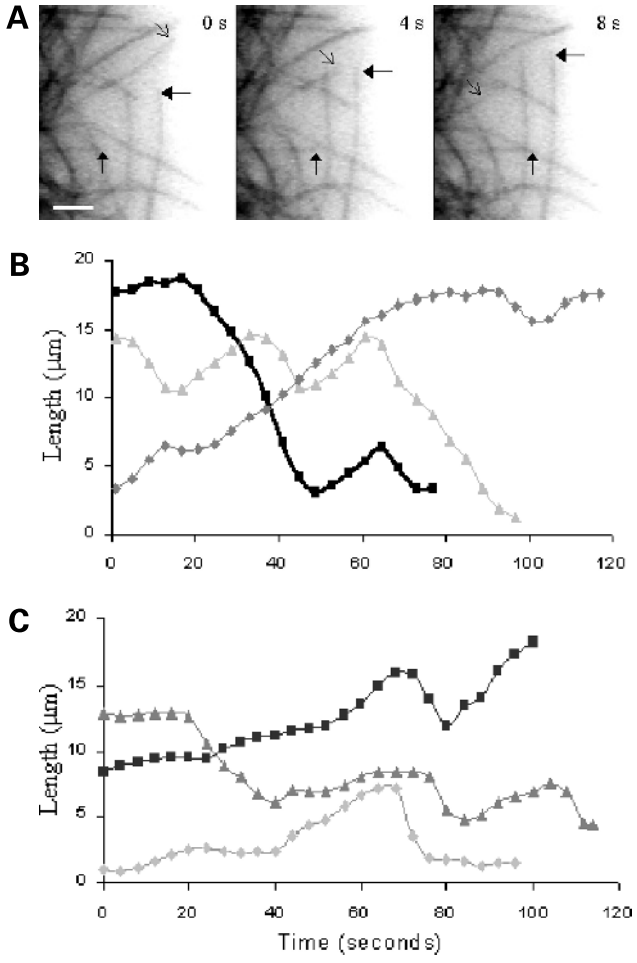

Figure 6. Time-lapse sequence of plus ends of fluorescent microtubules in a control MCF7 cell (**A**). Time is in seconds. *Bar*, 5 μm. The position of microtubule plus ends was tracked over time to generate life history plots in the absence (**B**) or presence (**C**) of 1 nmol/L E7389 from which microtubule dynamic instability variables were derived. Most microtubules in control cells grew (**A**, *solid arrows*) and shortened (**A**, *open arrows*) within the course of the 2-min observation period. In the presence of 1 nmol/L E7389 (**C**), microtubules grew more slowly and for shorter distances on average than control microtubules (**B**).

Microtubules were sufficiently dynamic for measurement in only eight cells. For this reason, we did not measure dynamic instability at 2 nmol/L E7389 because the results would reflect the behavior of only a small fraction of the microtubules. At 3 nmol/L E7389, the microtubules were partially depolymerized, and the increase in soluble tubulin obscured the ends of the microtubules (data not shown).

At Concentrations That Suppressed Microtubule Dynamics in Interphase, E7389 Arrested Mitosis and Altered the Organization of Mitotic Spindles

As shown in Fig. 7A, control cells in mitosis contained well-organized bipolar spindles with two distinct, well-separated spindle poles and a few astral microtubules. At metaphase, all of the chromosomes were organized in a compact equatorial metaphase plate. At 1 nmol/L E7389, which reduced interphase microtubule dynamicity by 28% (Table 1) and induced half-maximal mitotic accumulation, most spindles were bipolar but they contained some uncongressed chromosomes (Fig. 7B, *arrows*) and prominent astral microtubules. Some spindles were multipolar with highly disorganized chromosomes. Between 1 and 10 nmol/L of E7389, the mass of microtubules decreased, bipolar spindles were shorter than at the lower E7389 concentration (Fig. 7C), and the frequency of very abnormal mitotic cells containing many small asters of short stubby microtubules increased (Fig. 7D). The density of microtubules decreased in interphase cells at drug concentrations >2 nmol/L (compare Fig. 7E–H), but the overall organization of microtubules was unchanged from those in controls. The percentage of multinucleate interphase cells increased from 5% in controls to 16% to 23% at concentrations between 0.3 and 100 nmol/L E7389 (data not shown).

Discussion

E7389 inhibits microtubule growth, but not shortening, in association with sequestration of tubulin into unusual aggregates. At concentrations ≥100 nmol/L, the novel halichondrin analogue E7389 inhibited microtubule polymerization with MAP-depleted bovine brain tubulin *in vitro* in a concentration-dependent manner, and induced formation of globular tubulin aggregates 24 ± 6 nm in length and 14 ± 4 nm in width. Assuming the dimensions of a tubulin dimer to be 8 × 4 nm (28), each globular aggregate may contain on the order of 30 tubulin dimers. Many drugs and compounds that bind at or near the vinblastine-binding site and depolymerize microtubules at relatively high concentrations (vinblastine, cryptophycins, dolastatin 10, cemadotin, phomopsin A, hemiasterlin, diazonamide, and tubulysin A) also induce aggregation of tubulin, but, in contrast with E7389, the aggregates are in the form of rings, partial rings, or spirals (29, 30). Interestingly, the two published studies of the effects of these ''depolymerizing'' drugs on microtubule dynamic instability found that both vinblastine and cemadotin suppress the microtubule shortening rates and lengths, whereas E7389 does not. Thus, vinblastine and cemadotin both stabilize a ring-shaped filamentous tubulin structure whereas E7389 does not, indicating a different mode of interaction with the tubulin dimer. *In vitro* with purified microtubules, 100 nmol/L E7389 also suppressed the microtubule growth rates and lengths by 46% and 51%, respectively, more than twice the percentage of time in the phase of pause or attenuation, and suppressed the dynamicity by 40%.

E7389 induced mitotic arrest in association with inhibition of microtubule growth parameters, but with no effect on parameters of microtubule shortening. In living MCF7 cells in interphase, at the concentration that blocked mitosis half-maximally (1 nmol/L), E7389 significantly suppressed the microtubule growth rate, length, and duration by 27%, 50%, and 28%, respectively, and suppressed their overall dynamicity by 28%. Many antimitotic drugs and compounds (vinblastine, cryptophycins, nocodazole, estramustine, taxanes, noscapine, epothilone B, and discodermolide)

suppress the rate and extent of microtubule shortening and alter the frequencies of catastrophe and rescue (11, 23, 26, 31–37). In contrast, E7389 had little or no effect on these parameters *in vitro* or in cells (Table 1; Figs. 3 and 6).

The results suggest that mitotic block by microtubule-active drugs does not necessarily require suppression of microtubule shortening or catastrophe and rescue frequencies, but that suppression of microtubule growth events and overall dynamicity may be sufficient to produce abnormal spindle morphology and to suppress the metaphase/anaphase transition. In addition, a direct comparison of the ability of E7389 and vinblastine to suppress dilution-induced microtubule depolymerization *in vitro* (using drug concentrations that inhibited microtubule polymerization by 30%) indicated that E7389 was unable to stabilize MAP-rich microtubules against dilution (it was unable to reduce the tubulin off-rate constant) whereas vinblastine significantly suppressed dilution-induced depolymerization (Fig. 4). Thus, importantly, E7389 has no detectable stabilizing effect on microtubule ends at the concentrations that block mitosis or that significantly inhibit microtubule polymerization *in vitro* (by 30%).

We note that higher concentrations of E7389 were required for equivalent suppression of microtubule dynamics *in vitro* (100 nmol/L) as compared with in cells (1 nmol/L drug added to the medium). This discrepancy has often been observed with other antimitotic drugs including paclitaxel and *Vinca* alkaloids, and likely results from the uptake of E7389 into cells to levels severalfold higher than those in the medium, as previously shown for paclitaxel, colchicine, vinblastine, vinorelbine, and vinflunine (9, 13, 38).

Mechanism of Action of E7389

At steady state in cells or *in vitro*, dynamic microtubules are in equilibrium with a concentration of soluble tubulin called the ''critical concentration.'' In cells, ~35% to 60% of the tubulin is present in the form of microtubules, and the remainder, the critical concentration, is in dimeric (soluble) form (39, 40). All dynamics experiments reported here, both with purified microtubules *in vitro* and in cells, were done under steady-state conditions. Thus, even in the presence of the drug, the critical concentration of soluble tubulin dimers was maintained at normal levels. When tubulin is aggregated by a drug into an insoluble form that can no longer assemble into microtubules, microtubules depolymerize to reestablish the critical soluble tubulin dimer concentration. Thus, the inhibition we observed in growth rate and length could not have resulted from a decrease in availability of soluble tubulin, but must have resulted from a microtubule-binding mechanism. The inhibition may have resulted from blockage of the microtubule ends by binding of E7389 itself or tubulin-E7389 to the microtubule ends. Unliganded E7389 or tubulin-E7389 dimers or oligomers must transiently bind to the microtubule ends and ''poison'' or slow the addition of tubulin dimers to the microtubule end, thus reducing the growth rate. Oligomers were not visible by light microscopy in cells, but were prominent *in vitro* by electron microscopy; they would likely be undetectable in cells by electron microscopy.

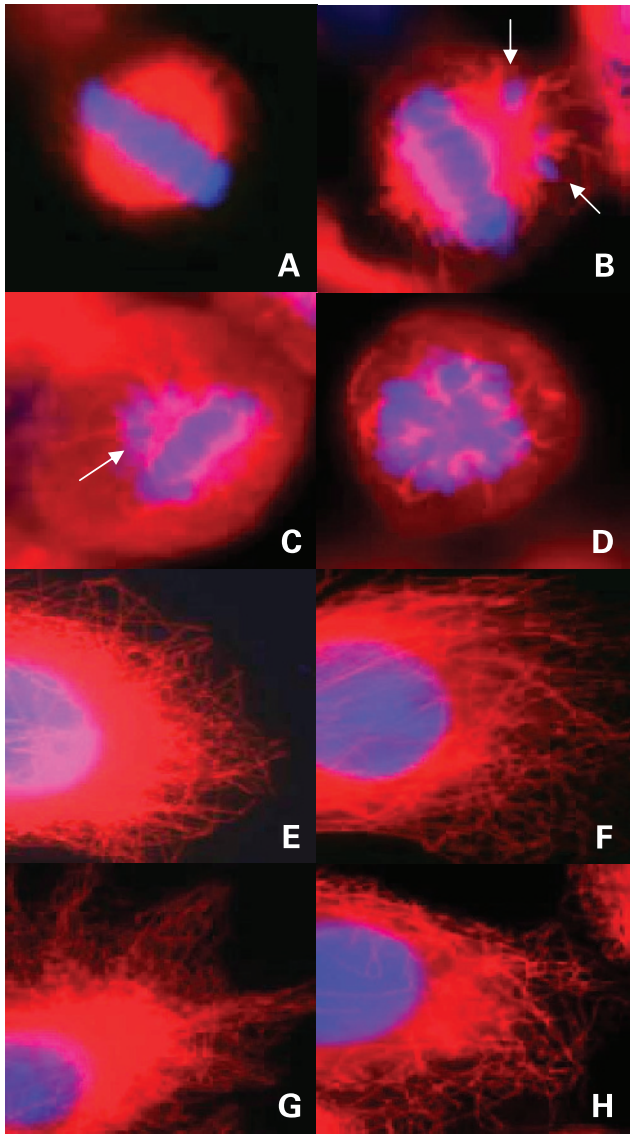

Figure 7. Concentration dependence for effects of E7389 (20 h incubation) on microtubule arrangements and spindle morphology in MCF7 cells. Chromosomes are blue (4′,6-diamidino-2-phenylindole) and microtubules are red (tubulin antibody; see Materials and Methods). **A**, metaphase spindle of control cell (no drug) is bipolar with all chromosomes congressed to the metaphase plate; **B**, at 1 nmol/L E7389, most spindles were bipolar with only a few chromosomes that remained at the poles and did not congress (*arrow*); **C**, 2 nmol/L E7389, spindles were noticeably shorter and contained many uncongressed chromosomes and prominent thick astral microtubules; **D**, 10 nmol/L E7389, as the drug concentration was increased, the frequency of severely abnormal mitotic cells containing many small asters of short stubby microtubules increased. Interphase cells (**E**, control; **F**, 1 nmol/L; **G**, 2 nmol/L; **H**, 10 nmol/L). In control cells (**E**) in interphase and at 1 nmol/L E7389 (**F**), the microtubules were very thin and densely distributed in a fine meshwork whereas at 2 nmol/L E7389 (**G**) microtubules were shorter and pulled back from the cell periphery, and at 10 nmol/L E7389 (**H**), the microtubules were very short, thick in diameter, and more sparsely distributed.

Many microtubule-targeted drugs, including vinblastine, colchicine, cryptophycin 52, and paclitaxel, can bind with relatively high affinity directly to microtubules, either to their ends, as with the first three drugs, or along their lengths, as with paclitaxel (10, 23, 32, 41, 42). Many drugs that bind directly to microtubules can stabilize the microtubule against shortening and significantly alter the catastrophe and rescue frequencies. For example, when an average of four molecules of cryptophycin 52 bind to the end of a microtubule, the microtubule shortening rate is diminished by 34%, the shortening length is reduced by 48%, the catastrophe and rescue frequencies (per minute) are increased by 35% and 25%, respectively, and the catastrophe and rescue frequencies (per length grown or shortened) are increased by 97% and 111%, respectively (32). E7389 did not affect these variables at low concentrations. Its effects at higher concentrations were not measurable due to the short length of the microtubules *in vitro* and to the large amount of background soluble tubulin in cells. The results suggest that E7389 or E7389-tubulin or the aggregates bind with low affinity to the microtubule ends, and thus the drug exerts its primary action on microtubule dynamics by transiently preventing addition of non-drug-bound tubulin dimers (free tubulin dimers) to the microtubule end and thus slowing growth.

Although E7389 binds to the vinblastine site on tubulin, it clearly acts differently from vinblastine as indicated by its ability to block mitosis without inhibiting microtubule shortening and by its inability to suppress microtubule depolymerization in dilution-induced disassembly experiments. Interestingly, two other *Vinca* alkaloids, vinflunine and vinorelbine, show some similarities to E7389 in their effects on microtubule dynamic instability. In *in vitro* studies comparing the effects on vinflunine, vinorelbine, and vinblastine on steady microtubule dynamic instability *in vitro*, Ngan et al. (31) found that vinflunine and vinorelbine suppressed microtubule growth rates similarly to vinblastine, but had no significant effect on microtubule shortening rates or durations. In contrast to E7389, vinflunine and vinorelbine both significantly increased the frequency of rescue. In addition, in MCF7 cells we have found that mitotic block by vinflunine is associated with inhibition of microtubule growth rates but not with shortening rates.[3] Suppression of shortening rates most likely requires that the drug induces a conformational change in the tubulin at the microtubule end that stabilizes the microtubule end or prevents a conformational change necessary to initiate shortening. Drugs like vinblastine impair microtubule dynamics by binding to the microtubule ends and by both sterically blocking further tubulin dimer addition and preventing or slowing the conformational changes required to initiate microtubule depolymerization. Vinblastine has been shown to induce a conformational change in tubulin that produces an isodesmic self-association of tubulin (43–45); thus, vinblastine clearly has pronounced effects on tubulin conformation.

How E7389 Arrests Mitosis

At 1 nmol/L E7389, mitotic spindles appeared similar to those in control cells with the exception that in many spindles, some chromosomes were unable to congress to the metaphase plate and remained at one pole and astral microtubules were prominent (compare Fig. 7A and B). The decrease in the microtubule growth parameters suggests that during prometaphase, in the presence of 1 nmol/L E7389, microtubules did not grow sufficiently to contact the kinetochores of chromosomes that were located far from one pole, and thus these chromosomes never attained a bipolar orientation in the spindle and continued to remain attached to only one pole, thus delaying or preventing anaphase (46, 47). At slightly higher concentration (2 nmol/L), spindle microtubules were clearly depolymerized and shorter (Fig. 7C). Microtubule dynamics were even more suppressed, and only 35% of the interphase cells had a significant number of microtubules that were detectably dynamic.

Interestingly, the nearly complete suppression of microtubule dynamics by E7389 in living interphase cells occurred over a very narrow drug concentration range. Thus, at 1 nmol/L E7389, the microtubule growth rate was suppressed by only 27%, whereas at 2 nmol/L, most interphase microtubules were minimally dynamic. The dynamics of microtubules in cells is regulated by a balance between microtubule-stabilizing and -destabilizing factors. It is conceivable that E7389-induced tubulin aggregates might also sequester microtubule-stabilizing and growth-promoting proteins [e.g., EB1 and $p150^{Glued}$ (48) or TOG (49)], effectively inhibiting microtubule growth both by forming E7389-bound tubulin oligomers and by inhibiting the actions of growth-promoting regulatory proteins. Taken together, the results indicate that E7389 acts by a novel mechanism that involves its ability to aggregate tubulin and selectively suppress microtubule growing events.

[3] K. Kamath, L. Wilson, and M.A. Jordan, unpublished data.

References

1. Hamel E. Natural products which interact with tubulin in the *Vinca* domain: maytansine, rhizoxin, phomopsin A, dolastatins 10 and 15 and halichondrin B. Pharmacol Ther 1992;55:31–51.

2. Bai RB, Paull KD, Herald CL, Malspeis L, Pettit GR, Hamel E. Halichondrin B and homohalichondrin B, marine natural products binding in the *Vinca* domain of tubulin. Discovery of tubulin-based mechanism of action by analysis of differential cytotoxicity data. J Biol Chem 1991; 266:15882–9.

3. Towle MJ, Salvato KA, Budrow J, et al. *In vitro* and *in vivo* anticancer activities of synthetic macrocyclic ketone analogs of halichondrin B. Cancer Res 2001;61:1013–21.

4. Kuznetsov G, Towle MJ, Cheng H, et al. Induction of morphological and biochemical apoptosis following prolonged mitotic blockage by halichondrin B macrocyclic ketone analog E7389. Cancer Res 2004;64: 5760–6.

5. Luduena RF, Roach MC, Prasad V, Pettit GR. Interaction of halichondrin B and homohalichondrin B with bovine brain tubulin. Biochem Pharmacol 1993;45:421–7.

6. Jordan MA, Wilson L. Microtubules as a target for anticancer drugs. Nat Rev Cancer 2004;4:253 – 65.

7. Jordan MA, Wilson L. Microtubule dynamics: mechanisms and regulation by microtubule-associated proteins and drugs *in vitro* and in cells. In: T Fojo, editor. Microtubules: Importance in Human Diseases and as Therapeutic Targets: Humana Press; 2004.

8. Mitchison TJ, Kirschner M. Dynamic instability of microtubule growth. Nature 1984;312:237 – 42.

9. Jordan MA. Mechanism of action of antitumor drugs that interact with microtubules and tubulin. Curr Med Chem Anti-Canc Agents 2002;2:1 – 17.

10. Jordan MA, Toso RJ, Thrower D, Wilson L. Mechanism of mitotic block and inhibition of cell proliferation by taxol at low concentrations. Proc Natl Acad Sci U S A 1993;90:9552 – 6.

11. Kamath K, Jordan MA. Suppression of microtubule dynamics by epothilone B in living MCF7 cells. Cancer Res 2003;63:6026 – 31.

12. Kelling J, Sullivan K, Wilson L, Jordan MA. Suppression of centromere dynamics by taxol in living osteosarcoma cells. Cancer Res 2003;63: 2794 – 801.

13. Ngan V, Bellman K, Hill B, Wilson L, Jordan M. Mechanism of mitotic block and inhibition of cell proliferation by the semisynthetic *Vinca* alkaloids vinorelbine and its newer derivative vinflunine. Mol Pharmacol 2001;60: 225 – 32.

14. Okouneva T, Hill BT, Wilson L, Jordan MA. The effects of vinflunine, vinorelbine, and vinblastine on centromere dynamics. Mol Cancer Ther 2003;2:427 – 36.

15. Yvon A-M, Wadsworth P, Jordan MA. Taxol suppresses dynamics of individual microtubules in living human tumor cells. Mol Biol Cell 1999;10: 947 – 9.

16. Jordan MA, Wendell KL, Gardiner S, Derry WB, Copp H, Wilson L. Mitotic block induced in HeLa cells by low concentrations of paclitaxel (Taxol) results in abnormal mitotic exit and apoptotic cell death. Cancer Res 1996;56:816 – 25.

17. Kung AL, Zetterberg A, Sherwood SW, Schimke RT. Cytotoxic effects of cell cycle phase specific agents: result of cell cycle perturbation. Cancer Res 1990;50:7307 – 17.

18. Wang T, Wang H, Soong Y. Paclitaxel-induced cell death: where the cell cycle and apoptosis come together. Cancer 2000;88:2619 – 28.

19. Littlefield BA, Palme MH, Seletsky BM, Towle MJ, Yu MJ, Zheng W. Macrocyclic analogs and methods of their use and preparation. Vol. US Patent 6,214,865;2001.

20. Panda D, Miller HP, Wilson L. Rapid treadmilling of MAP-free brain microtubules *in vitro* and its suppression by tau. Proc Natl Acad Sci U S A 1999;96:12459 – 64.

21. Bradford MM. A rapid and sensitive method for the quantitation of microgram quantities of protein utilizing the principle of protein-dye binding. Anal Biochem 1976;72:248 – 54.

22. Panda D, Goode BL, Feinstein SC, Wilson L. Kinetic stabilization of microtubule dynamics at steady state by tau and microtubule-binding domains of tau. Biochemistry 1995;34:11117 – 27.

23. Derry WB, Wilson L, Jordan MA. Substoichiometric binding of taxol suppresses microtubule dynamics. Biochemistry 1995;34:2203 – 11.

24. Toso RJ, Jordan MA, Farrell KW, Matsumoto B, Wilson L. Kinetic stabilization of microtubule dynamic instability *in vitro* by vinblastine. Biochemistry 1993;32:1285 – 93.

25. Walker RA, O'Brien ET, Pryer NK, et al. Dynamic instability of individual microtubules analyzed by video light microscopy: rate constants and transition frequencies. J Cell Biol 1988;107:1437 – 48.

26. Panda D, Jordan MA, Chin K, Wilson L. Differential effects of vinblastine on polymerization and dynamics at opposite microtubule ends. J Biol Chem 1996;271:29807 – 12.

27. Wilson L, Snyder KB, Thompson WC, Margolis RL. A rapid filtration assay for analysis of microtubule assembly, disassembly, and steady-state tubulin flux. In: Wilson L, editor. Methods in Cell Biology 1982. p. 159 – 62.

28. Burns RG, Surridge CD. Tubulin: conservation and structure. In: Hyams JS, Lloyd CW, editors. Microtubules. NY: Wiley-Liss; 1994. p. 3 – 31.

29. Hamel E, Covell DG. Antimitotic peptides and depsipeptides. Curr Med Chem Anti-Canc Agents 2002;2:19 – 53.

30. Bai R, Taylor GF, Schmidt JM, et al. Interaction of dolastatin 10 with tubulin: induction of aggregation and binding and dissociation reactions. Mol Pharmacol 1995;47:965 – 76.

31. Ngan VK, Bellman K, Panda D, Hill BT, Jordan MA, Wilson L. Novel actions of the antitumor drugs vinflunine and vinorelbine on microtubules. Cancer Res 2000;60:5045 – 51.

32. Panda D, DeLuca K, Williams D, Jordan MA, Wilson L. Antiproliferative mechanism of action of cryptophycin-52: kinetic stabilization of microtubule dynamics by high affinity binding of microtubule ends. Proc Natl Acad Sci U S A 1998;95:9313 – 8.

33. Panda D, Himes RH, Moore RE, Wilson L, Jordan MA. Unusually potent suppression of microtubule dynamics by cryptophycin 1: a mechanism for its antiproliferative action. Biochemistry 1997;42: 12948 – 53.

34. Panda D, Miller H, Islam K, Wilson L. Stabilization of microtubule dynamics by estramustine by binding to a novel site in tubulin: A possible mechanistic basis for its antitumor action. Proc Natl Acad Sci U S A 1997; 94:10560 – 4.

35. Panda D, Singh JP, Wilson L. Suppression of microtubule dynamics by LY290181. J Biol Chem 1997;272:7681 – 7.

36. Vasquez RJ, Howell B, Yvon A-MC, Wadsworth P, Cassimeris L. Nanomolar concentrations of nocodazole alter microtubule dynamic instability *in vivo* and *in vitro*. Mol Biol Cell 1997;8:973 – 85.

37. Honore S, Kamath K, Braguer D, Wilson L, Briand C, Jordan MA. Suppression of microtubule dynamics by discodermolide by a novel mechanism is associated with mitotic arrest and inhibition of tumor cell proliferation. Mol Cancer Ther 2003;2:1303 – 11.

38. Jordan MA, Wilson L. The use and action of drugs in analyzing mitosis. In: Methods in Cell Biology: Academic Press; 1999. p. 267 – 95.

39. Jordan MA, Thrower D, Wilson L. Mechanism of inhibition of cell proliferation by *Vinca* alkaloids. Cancer Res 1991;51:2212 – 22.

40. Zhai Y, Borisy GG. Quantitative determination of the proportion of microtubule polymer present during the mitosis-interphase transition. J Cell Sci 1994;107:881 – 91.

41. Skoufias D, Wilson L. Mechanism of inhibition of microtubule polymerization by colchicine: Inhibitory potencies of unliganded colchicine and tubulin-colchicine complexes. Biochemistry 1992;31:738 – 46.

42. Jordan MA, Wilson L. Kinetic analysis of tubulin exchange at microtubule ends at low vinblastine concentrations. Biochemistry 1990; 29:2730 – 9.

43. Na GC, Timasheff SN. Thermodynamic linkage between tubulin self-association and the binding of vinblastine. Biochemistry 1980;19: 1347 – 54.

44. Na GC, Timasheff SN. Stoichiometry of the vinblastine-induced self-association of calf brain tubulin. Biochem Soc Trans 1980;8:1347 – 54.

45. Lobert S, Correia J. Energetics of *Vinca* alkaloid interactions with tubulin. In: Methods in Enzymology; 2000. p. 77 – 103.

46. Rieder C, Schultz A, Cole R, Sluder G. Anaphase onset in vertebrate somatic cells is controlled by a checkpoint that monitors sister kinetochore attachment to the spindle. J Cell Biol 1994;127:1301 – 10.

47. Rieder CL, Cole RW, Khodjakov A, Sluder G. The checkpoint delaying anaphase in response to chromosome monoorientation is mediated by an inhibitory signal produced by unattached kinetochores. J Cell Biol 1995; 130:941 – 8.

48. Ligon LA, Shelly SS, Tokito M, Holzbaur EL. The microtubule plus-end proteins EB1 and dynactin have differential effects on microtubule polymerization. Mol Biol Cell 2003;14:1405 – 17.

49. Spittle C, Charrasse S, Larroque C, Cassimeris L. The interaction of TOGp with microtubules and tubulin. J Biol Chem 2000;275:20748 – 53.